

The Ji-Ji, Taiwan Earthquake of 21 September 1999



Editor: Alan Stewart

EEFIT gratefully acknowledges the support of its corporate members:

Arup Group

British Geological Survey

CREA Consultants

Giffords

Halcrow

Risk Management Solutions

Sellafield Ltd

Sir Robert McAlpine

Earthquake Engineering Field Investigation Team

Institution of Structural Engineers

11 Upper Belgrave St

London

SW1X 8BH

United Kingdom

Tel: +44 (0)207 235 4535

Fax: +44 (0)207 235 4294

www.eefit.org.uk

© EEFIT 2007

ISBN 978 1 906335 10 6

1. Introduction

A magnitude 7.6 earthquake struck Taiwan at 01.47 local time on 21 September 1999. The epicentre was approximately 7km north west of Ji-Ji, a small town bordering a mountainous area some 155km south of Taipei, the capital. Ground shaking lasted around 40 seconds, and approximately 2,500 people were killed and 11,000 injured. Around 10,000 buildings were destroyed, with the same again being seriously damaged.

Damage was greatest in the central regions of Nantou, Taichung and Yunlin, and economic loss has been estimated at US\$10 to \$12 billion.

This was the largest earthquake to hit Taiwan since a magnitude 7.1 event of 1935 which killed around 3,500 people.

An EEFIT team visited the area three weeks after the event, and this short report provides a summary of their observations.

2. Tectonic Setting

Taiwan lies on the boundary between the Eurasian and Philippine Sea plates and has been created as the Philippine Sea plate moves north-westward at around 7cm a year. The collision area is marked by a north east trending zone of thrust and strike-slip faulting, and the earthquake occurred on the Chelungpu thrust fault near the centre of this zone.

The earthquake history of the island has been dominated by large magnitude earthquakes in the eastern part of the country, with less frequent shallow events in the western area where the 1999 event occurred. Only five of 43 recorded 20th century earthquakes were surface fault events like that of 21 September 1999, and much of the west of the island was therefore categorised as only moderately seismic.

2.1 Fault Movements

This earthquake was characterised by spectacular fault movements. At places the vertical lift was measured to be close to 10m. Such large fault movements were induced due to the nature of the thrust fault. Due to these large fault movements some of the civil engineering structures suffered quite badly. A few examples are presented below:



Figure 1: Fault movement caused this spectacular lift of this building that straddled across the fault



Figure 2: The building next to the one seen in the figure before suffered damage but survived without collapse



Figure 3: The athletic track at Wu Fang School suffered badly due to fault movements



Figure 4: Collapsed Wu Fang school building close to the athletic track



Figure 5: Where fault movements were smaller, bridges survived collapse



Figure 6: Failure of the dam due to fault movement (right hand side was uplifted by the earthquake)



Figure 7: Left hand edge of the dam which indicates the original level of the dam crest

Following the above observations there was a move in Taiwan to legislate against construction of buildings close to the known fault lines. Of course, not all fault lines have surface expression and some faults may be below ground and undetectable. The 921 Ji-Ji earthquake itself occurred on a less known Chelungpu fault which did not show much activity in the recent past.

3. Geotechnical Observations

3.1 Liquefaction phenomena

Liquefaction phenomena were observed at several locations in the Taichung area.

Figures 8 and 9 show a block of single storey houses in the suburbs of Yuan Lin city which suffered extensive liquefaction. The buildings settled and liquefied soil flowed into the rooms through the floor slabs, filling the rooms and lifting the furniture.

A nearby well was filled with liquefied soil flowing from the sub-strata (Figure 10), and eye witness accounts suggest that immediately following the earthquake there was high pressure ejection of soil from the sub-strata.



Figure 8: Single floor tiled roof house suffers settlement following liquefaction of sub-strata



Figure 9: A view inside the house showing the inflow of sub-strata filling the room and lifting the furniture



Figure 10: Well filled by liquefied soil

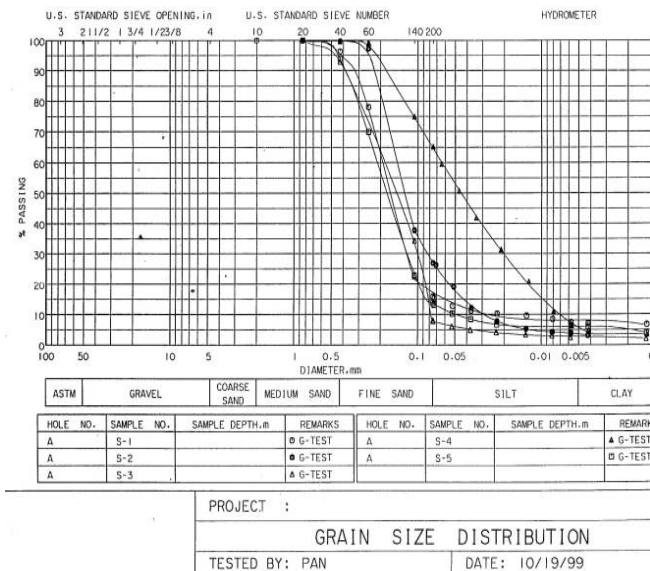


Fig.11: Particle size distribution of soil from the well in Fig.10, (courtesy A J Brennan, Research Student, Cambridge University)

Fig. 11 shows the particle size distribution of the soil samples collected from the well site, which confirm that the sub-strata consisted of fine grained sandy soils, which are susceptible to liquefaction. Following the EEFIT visit to this site, data was also obtained from bore samples in the area, and the sub-strata interpreted as shown in Fig.12. This indicates that the top soil layer consisted of clayey soil, with liquefiable layers below. It therefore seems likely that the excess pore water pressures generated in the sub-strata were initially retained by the upper clayey soil, leading to a sudden burst into the floor slabs of the houses and the well and an outflow of the material from the sub-strata.

A nearby factory compound displayed sand boils and mud volcanoes in the open compound. The factory floor slabs also exhibited classical yield line patterns (Figure 13), indicating that the ground below suffered settlement following liquefaction, offering little support to the floor slabs and causing them to fail.

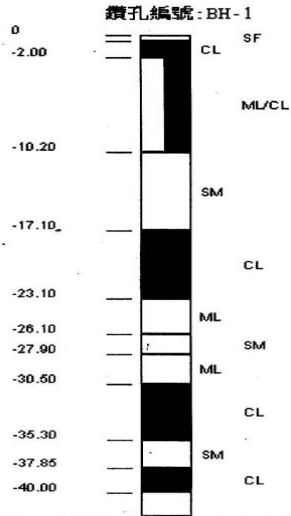


Fig.12 Soil classification based on bore hole data



Figure 13: Yield lines in floor slab

3.2 Liquefaction induced settlement

In Yuan Lin city, there were many buildings which suffered liquefaction induced settlements. Figure 14 shows rotation of a three storey building towards its neighbour. Figure 15 shows the settlement of this building relative to the road level, while Figure 16 shows a column breaking away from the floor slab at foundation level.



Figure 14: Building rotation due to differential settlement following liquefaction of the foundation soil

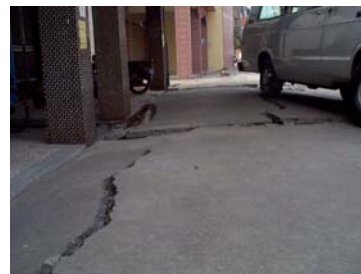


Figure 15: Settlement of the ground floor relative to road level



Figure 16: Settlement of a column at the foundation

There were many examples of liquefaction induced settlement and the figures above illustrate typical examples. In general the structural damage suffered by these buildings was relatively minor and therefore it is fair to say that these are geotechnical failures.

3.3 Lateral spreading

When liquefaction of soil occurs either in the body of, or underneath, a slope, the ground will exhibit lateral spreading. Even gentle slopes of 3° to 6° to the horizontal are known to suffer lateral spreading.

There were many examples of lateral spreading in this earthquake, and a typical example is at the site of a new bridge near Nantou city, shown in Figure 17. Liquefaction of the soil was very obvious at this site with sizeable sand boils visible on the ground surface, examples of which are shown in Figure 18.



Figure 17: Lateral spreading of the slopes parallel to abutments showing deep tensile cracks



Figure 18: Sand boils at the new Nantou Hsou-Shi bridge site

3.4 Landslides

Taichung and neighbouring districts witnessed landslides on a massive scale, resulting in major destruction of the overgrowth, as shown in Figure 19.



Figure 19: Landslides causing loss of over growth



Figure 20: Blocking of hill roads due to landslides

By and large, the land slides seem to have occurred at fairly shallow depth, and were not deep seated slope failures. A shallow depth of the top soil has suffered slippage causing the tree and plant debris to slide downhill thereby exposing the soil layers below. Figure 20 shows blockage of the hill roads, which was a common result, leading to a loss of communication between Taichung city and interior villages.

The performance of tunnels following the earthquake was mixed. Figure 21 shows one such tunnel which suffered structural damage to its lining. However, the tunnel was located in a hill side which suffered landslides with material from the top of the slope sliding parallel to the tunnel axis. It was therefore not clear whether the damage to the tunnel lining was due to the earthquake loading causing additional stresses in its lining or due to material flow close to the tunnel crest. The tunnel was leaking water and the road was blocked off by the authorities.



Figure 21: Tunnel located in the side of a hill with landslides at the surface



Figure 22: Landslides caused failure of the lifelines laid next to the roadway



Figure 23: Reinforced slope failure

The landslides also caused to damage to the lifelines laid next to the road way. In Figure 22, the re-laying of new lifelines can be seen.

3.5 Reinforced slope failure

The earthquake provided an example of the performance of a reinforced slope. The slope is located at the campus of the National Chihnan University of Information, and is approximately 120 m high, with failure occurring over a width of about 300 m. Figure 23 shows the failure.

A polyethylene cover had been placed on the upper reaches of the slope after the earthquake, to prevent further sliding due to rain water seeping into the slope. The slope angle is very steep and was estimated at approximately 70° . As a result a reinforcement was used which consisted of geotextiles and geonets. The geotextile appeared to have been laid horizontally and was wrapped around a geonet filled with locally available material (rocks plus coarse sand) similar to the rock filled wire mesh gabions used in the UK to stabilise slopes. The geotextile was anchored to a depth of about 2m into the slope. The slope appeared to be well designed with adequate drains at regular intervals running horizontally and well connected to vertical drains running down the slope. However, it is not known whether the slope was designed to sustain dynamic earth pressures generated during the earthquake.

The failure of this reinforced slope was mainly due to pull out of the geotextile from its embedment. The geotextile was 'pushed out' by the material in the slope flowing downwards and outwards, and Figure 24 shows the freely hanging geotextile. The gabions made from geonets simply moved out with the geotextile as seen in Figure 25, although at some locations the geotextiles showed clear signs of tensile failure as shown. It may be possible to investigate whether such failures can be avoided by increasing the geotextile anchorage depth.



Figure 24: At some locations, the geotextile failed in tension



Figure 25: The wrapping of the Geotextile around Geonet gabions filled with was pulled out en bloc

4. Buildings and Structures

4.1 Building Codes and Building Form

The Taiwan Building Code (TBC) was revised in 1974, 1982 and 1996, and it seems that the majority of the affected buildings would have fallen within the remit of the 1982 revision. This required ductile detailing of r.c. frame buildings in a similar manner to the US Uniform Building Code (UBC) of the time. The later 1996 revision is broadly consistent with the 1994 UBC. The epicentre occurred in the "moderate" seismic zone.

Buildings over 50m (around 15 stories) require a special peer review process during planning approval, with the result that many buildings stop just short of this height.

In rural areas the traditional form of construction has been of unreinforced masonry or adobe with timber roofs.

Most urban structures are built of reinforced concrete, with structural steel adopted for tall buildings. Unreinforced brick walls and infill panels are common, even in recent construction. Figure 26 shows typical construction.



Figure 26: Typical urban construction of a reinforced concrete frame with brick infill

Arcade style buildings are also a common feature, with open shop fronts at ground level and a projecting floor above to create a covered pedestrian walkway. Many are three or four stories high, but 12 stories is not uncommon. Until recently many cities encouraged this style of construction. However, it commonly creates an undesirable soft storey, and many buildings of this type collapsed. Several observers have noted that few buildings with brick infill at ground level collapsed, although they might be severely damaged.

Figure 27 shows a typical open shop front; loss of concrete cover at top and bottom of the columns is noticeable, but in this case the building has survived. Figure 28 shows typical shear cracking of internal walls



Figure 27: Typical Open Shop Front



Figure 28: Shear Cracking of Internal Walls

A number of common failure modes were evident. Figure 29 shows loss of cover concrete at a beam/column interface. However, it can be seen that there is closely spaced confinement reinforcement in the column in the potential hinge area immediately below the beam and this area of the building structure has remained standing.

However, Figure 30 shows another column of the same building, where lack of confinement has permitted serious damage and partial collapse of this area of the building.



Figure 29: Loss of Cover at Beam/Column Interface



Figure 30: Lack of Confinement at Column Head

Figure 31 shows a soft storey failure, with the building now propped as an emergency measure. A failed column is visible in left centre, and the small amount of main reinforcement is striking, as is the absence of adequate confinement. Figure 32 shows another example, this time in a part complete building. The form of construction here, with part height concrete infill walls, gives rise to a very much softer storey at ground level. Again, a detached column with very limited reinforcement is visible in the foreground.



Figure 31: Soft Storey Failure



Figure 32: Soft Storey Failure

4.2 Public Buildings

Some 50 schools were reported as completely destroyed and 700 damaged. Fifty one police stations were also reported as being destroyed, with 10 fire stations said to be seriously damaged.

There are 165 hospitals in the surrounding area, and varying amounts of damage occurred. It is reported that 1,000 beds were lost in Nantou county alone, and several facilities made recourse to tents erected in the grounds.

Non-structural damage such as equipment failure, collapsed ceilings and flooding from pipe leakage were often significant constraints on functionality.

Chi-Nan University in Puli was badly damaged and students were relocated.

4.3 Industrial Facilities

In general, damage to industrial facilities was relatively light and initial concerns over the effect on Taiwan's semiconductor production facilities proved largely unfounded on this occasion.



Figure 33: Collapsed Silos

However, there were many reports of damage to aggregate and concrete plants, with silos of heavy materials collapsing and damaging surrounding plant. Figure 33 shows one such example.

Sloshing of the contents of molasses storage tanks at Taichung port caused significant tank damage as shown in Figure 34, while Figure 35 shows settlement of pipeline supports due to ground liquefaction.



Figure 34: Tank Damage at Taichung Port



Figure 35: Pipeline Settlement Through Ground Liquefaction

5. Lifelines

All the major lifelines were disrupted by the earthquake.

5.1 Bridges

Thirty bridges were reported as sustaining damage, including five which collapsed.

Figures 36, 37, 38 show structural failures of bridge piers; note the light reinforcement in Figure 38.



Figure 36: Bridge Pier Failure from Transverse Acceleration



Figure 37: Shear and Transverse Displacement of Bridge Piers



Figure 38: Close Up of Bridge Pier Reinforcement

There were also many examples of soil-structure interaction in this earthquake affecting bridges. An example is a bridge near Taiping city, shown in Figures 39 and 40. This bridge site is very close to the fault line which showed vertical movements of about 3 to 4 metres and lateral movements of about 1 to 2m. The bridge structure itself was in the process of being widened at the time of the earthquake, with new piers being constructed.

It is therefore interesting to compare the behaviour of the original and new construction.

The old bridge suffered total damage with decks falling off the bearing pads on the supporting piers. The pier rotation was largely driven by the deck movements as seen in Figure 39. In Figure 40 the new bridge pier with no bridge deck in place can be seen in the foreground. This pier has suffered rotations in the opposite direction compared to the old bridge piers. This example illustrates the dynamics of the bridge deck, bridge pier and the foundation soil system.



Figure 39: Rotation of the old bridge piers due to deck movements



Figure 40: The new piers with no bridge deck suffered rotation in the opposite direction

With the inertia of the bridge decks driving the movements the old piers were forced to rotate due to the lateral inertial forces being applied by the deck. The foundation soil appeared to be silty sand in a fully saturated state owing to the proximity of the river (see Figure 40). As a result, there would have been some excess pore water pressure generation, leading to a degradation of its stiffness. Unable to resist the moment being applied by the deck, the foundation block supporting the pier simply rotated in an anti-clockwise direction. The new bridge pier with no load on the top had an opportunity to undergo free vibrations. With the foundation soil softening it suffered differential settlements and rotated clockwise. Full liquefaction was obviously not realised as the overall settlement of both the old and new bridge piers seem to be small.

Figure 41 shows a bridge near Nantou city while Figure 42 shows a close up of the far abutment, which was completely destroyed. Lateral spreading was also very clearly evident at the base of the bridge piers. Local enquiries confirmed that the piers were designed to modern standards and were founded on deep piles carrying loads to competent bed rock.



Figure 41: Overview of the bridge and the piers, the abutment on the far side was destroyed as seen in Figure 42



Figure 42: Bridge abutment completely destroyed

Figures 43 and 44 show the soil flow at the base of the piers. As the soil flow towards the river is obstructed by the pier, there was a ground heave observed in the regions behind the piers.



Figure 43: Soil flow obstructed by the pier causes a ground heave behind the pier



Figure 44: Close up view at the base of the pier showing the original mark of the pier before lateral spreading

In Figure 45 the approach roads are seen to have settled relative to the bridge deck. This is consistent with the fact that the piled foundations and piers supported the deck well and consequently no settlement of the deck was visible.



Figure 45: Settlement of the approach roads relative to the bridge deck



Figure 46: Precarious rotations of the old bridge piers, pressed into action to ferry materials to repair the new bridge abutment

Figure 46 shows the piers of an old bridge, which was brought into use following the failure of the abutments and approach roads of this new bridge. The piers of the old bridge show extensive rotation, confirming the lateral spreading at this site.

5.2 Electrical Power Systems

Although it seems that generating capacity remained largely operational, there was significant damage to substations and to the transmission system (Figures 47 and 48). However, the Taiwan Power Company did anticipate restoring virtually all supply within a month of the earthquake.



Figure 47: Typical Transmission Tower Damage



Figure 48: Damaged Substation

5.3 Water Supply

It is estimated that there are 5 million water consumers in the region, and around 80% suffered some disruption of supply. The most spectacular effect, widely reported, was failure of the Shih-kang dam, some 50km from the epicentre, which supplied about half the water for the area. The fault passed through one end of the dam, and the vertical ground movement of 10m caused collapse of that end of the dam (Figures 49 and 50).



Figure 49: Shih-Kang Dam



Figure 50: Shih-Kang Dam

5.4 Ports

Taichung port was significantly affected by liquefaction, with numerous sink holes appearing. The quay walls also moved slightly, with the ground behind them reported to have settled up to 2m. Figures 51, 52 and 53 show typical damage.



Figure 51: Taichung Port



Figure 52: Taichung Port



Figure 53: Taichung Port

6. Conclusions

Sadly, the causes of the damage that EEFIT witnessed on this field mission are all too common; poorly designed and detailed structures, insufficient consideration of soil-structure interaction, and poorly sited structures. All of the major damage seen was preventable by appropriate application of the relevant design codes and no unusual or inexplicable damage was noted.

Acknowledgements

EEFIT would like to thank EPSRC, which funded the academic staff on the mission, and the various employers who funded the industry staff. Without such support, EEFIT missions would not be possible. EEFIT would also like to thank the many organisations and individuals in Taiwan who gave freely of their time to assist the mission.

Geotechnical photos and text by Gopal Madabhushi, University of Cambridge; structural photos courtesy of David Edge, Atkins.